Proceedings of the 2nd International Conference on Fluid Flow, Heat and Mass Transfer
Ottawa, Ontario, Canada, April 30 – May 1, 2015
Paper No. 157

Comparative Study on Flow Control in the Cylindrical S-Shaped Duct with Parallel and Angled Vortex Generator

Tayebeh Fahimivala, Roholah Ghodsi
Islamic Azad University, Department of Aerospace Engineering
Garmsār, Semnan, Iran
Tayebeh.fahimivala@gmail.com; dr.sr.ghodsi@ut.ac.ir

Abstract- Air entrance efficiency directly affects the engine efficiency. Given the importance of the air entrance duct for the jet engine and the plane's performance, once the duct prototype is designed and built, it is necessary to extensively investigate it to obtain the best air entrance duct. The main purpose of the present research was to study the general flow behaviour in an S-shaped duct and the application of a vortex generator to control the flow separation area inside the duct. For this purpose, An S-shaped air entrance (M2129) was used. The simulations were performed in a base mode (without vortex generator) and two vortex generator configurations with parallel and angled blades. Results showed that vortex generator almost eliminated the separation area and reduced total pressure drop, and consequently, increased engine efficiency. The results of the simulation indicated that utilizing a parallel vortex generator can increase total pressure recovery from 96.65% to 97.08%.

Keywords**:** S-duct diffuser, Air-intake, Computational fluid dynamic (CFD), Turbulence models, Vortex generator (VG)

Nomenclature

D_{throat} : *Throat diameter*
D_{EF} : *Diameter at engine face*
L_D : *Duct length*
α_1 : *Angle of attack*
P_s : *Static pressure inlet*
T_t : *Total temperature inlet*
T_s : *Static temperature inlet*
η : *total pressure recovery*
P_{tao} : *total pressure Average in the outlet section* (pa)
P_{tao} : *total pressure Average in the inlet section* (pa)
C_a : *Air speed*
P_t : *Total pressure inlet*
Re : *Reynolds number*
t : *Maximum thickness*
α : *Angle of attack*
β : *angle between the blades*
C : *Blade length*
h : *Blade hight*
L : *Distance of blades*
+VG : *with vortex generator*
–VG : *without vortex generator*
+VGP : *with parallel vortex generator*
+VGA : *with angled vortex generator*
P_f : total pressure average at outlet section
P_i : total pressure average at inlet section

1. Introduction

Aircraft propulsion systems often utilize the S-shaped subsonic ducts as their air intakes. The main reason for using the S-ducts is to provide an ambient air source from above the wing and the fuselage for the engine compressor.

In other words, it converts the kinetic energy of the free stream to the static pressure in the compressor section. The duct should be designed in such a way that the free stream velocity decreases smoothly and slowly and causes an increased static pressure with uniform stream distribution in the compressor section. The flyer Mach number increases, the entrance duct design becomes more complex

and critical. The entrance duct efficiency directly affects the engine performance and trust. The highest trust is obtained when the entrance duct transfers the required air of the engine with the highest total pressure to the compressor section. Bended air intakes are utilized by designers in all flight regimes. Dual-bended (S-shaped) air intakes are widely-used by engine designers as they meet design requirements (e.g. radar evasion and motor installation location) and have an acceptable performance.

S-shaped diffusers have a central curvature and an increased cross-sectional area in the flow direction. The central curvature creates a lateral pressure gradient, which in turn, creates secondary flows. The lateral flow also results in a non-uniform pressure distribution in the entrance plane of the duct. Additionally, the pressure gradient in the flow direction can cause flow separation due to the increased section area. A well-designed S-shaped air intake should be able to reduce the inflow.

To achieve a suitable efficiency in an S-shaped duct, it must have the minimum total pressure loss and a flow almost uniform with small lateral velocity components along the duct. Limitations on the size and weight of the airplane make designers use shorter air intakes which results in an increased curvature and an inverse pressure gradient. Therefore, it is important to control the flow inside the bended air intakes.

The first reports on preventing the rotation of the flow inside of S-shaped air intake at different angles of attack were presented by Guo, R. W., & Seddon, J. (1983). They used spoiler to reduce flow distortion at high angles of attack. Lin, J. C. (1991) experimentally studied various equipment that generated a vortex. Reichert, B. A., & Wendt, B. J. (1993) used short-profile vortex generators (VGs) to improve total pressure distortion and recover the efficiency of an S-shaped duct. They, in another study Reichert, B. A., & Wendt, B. J. (1994), used 20 different configuration of the cone-shaped vortex generators to reduce distortion and improve total pressure recovery in an S-shaped diffuser. The best configuration was able to reduce distortion by up to 50% while the improvement in pressure recovery was about 0.5%. Sullerey (2002) conducted experiments to examine the effects of fences and vortex generators in reducing the distortion in the outlet and improving pressure recovery in an S-shaped 2-D entrance duct. It was observed that fences and vortex generators perform better in smaller and larger curvature ratios, respectively.

2. S-duct Geometry

As mentioned before, the S-shaped duct entrances are commonly used. This type of entrance (the M2129 type) was used in the present research too. Eqs. (1) - (2) show the central curvature line equation and the distribution of the duct section, According to Berens. (2012). The geometry parameters and the duct shape are shown in Table 1 and Fig. 1, respectively. It should be noted, for a Scrutiny of results in the duct, perpendicular planes created in the direction of flow. These pages are: sec.1 (At the beginning of the separation), sec.2 (In the curvature of duct) and sec. 3 (At the end of separation and the engine entrance).

$$z = 0, x = -0.15L(1.0 - \cos(\frac{\pi x}{L_D})) \tag{1}$$

$$D = D_{throat} + (D_{EF} - D_{throat})(3.0(1 - \frac{x}{L_D})4 - 4.0(1.0 - \frac{x}{L_D})3 + 1.0) \tag{2}$$

Table 1. Description of important duct parameters.

D_{throat}	D_{EF}	L_D
0.1288 m	0.1440 m	0.4572 m

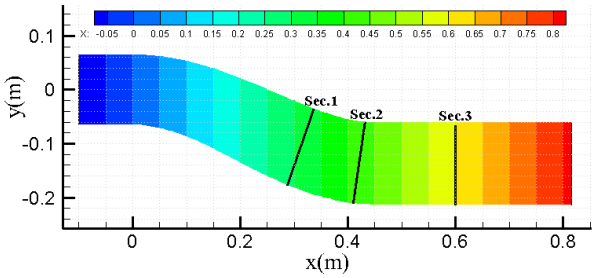

Fig. 1. Duct Geometry and Sections perpendicular to the Flow direction

3. Numerical Solution Method & Boundary Conditions

Navier-Stokes equations were solved through control volume scheme using the pressure base method. Convection Terms were discretized using the up-wind second order method, and turbulence were modeled using the Spalart-Allmaras turbulence method. The equations are described in detail in P. Spalart and S. Allmaras. (1992) and Dacles-Mariani. (1995).

4. Grid Independency and Validation

The grid generation principles were all considered. The grid generation of duct was done using the structure model with a boundary layer near the wall and blocks in regions farther from the wall, Jin, Wonjin. (2008). Fig.2 shows an example of perpendicular grid planes in the direction of flow and a produced boundary layer, respectively. To examine the grid independency, 220,000, 487,000, and 1,900,000 volume cells were investigated for a duct without the vortex generators. All boundary conditions were considered according to Berens. (2012) when examining the grid independency, validating and comparing the results in the case without the vortex generators (Table 2).

As shown in Table 3, the difference between mass flow rate percentages decreased to 0.68% after refining the grid to 487,000 elements. This means that with this number of cells, results were almost independent of the computational grid, and the grid could be used with certainty for validation.

Table 2. Boundary and inlet Condition for S-duct According to Jin, Wonjin. (2008).

parameter	Value
M	0.207
C_1	335.54 m/s
U	69.46 m/s
α_1	0 Deg.
P_t	103051.07 pa
P_s	100018.18 pa
T_t	282.6 k
T_s	280.2 k
ρ_a	1.243745 kg/m3
$\dot{m}$	2.8727 kg/s
Re	4932254

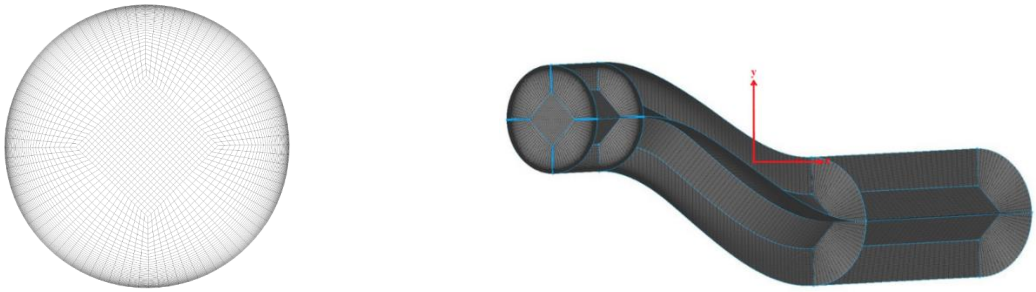

Fig. 2. Quality and management of mesh in the duct.

Table 3. Number of volume cells for mesh independency

Number of volume cells	Mass flow rate (kg/s)	Diff (%)
220e3	2.70	-
487e3	2.86	5.59
190e4	2.88	0.69

Validation of the obtained results with authentic references is an important factor in research. To validate the results, the non-dimensional pressure (p / p_{t_ref}) was compared to the computational results and the experimental data along the duct. Fig.3 shows the non-dimensional pressure distribution along the duct and its comparison with the computational and experimental data for the starboard and port walls. As seen in the figures, an acceptable agreement was observed between the obtained results and the experimental results and the RANS numerical model presented in Berens. (2012).

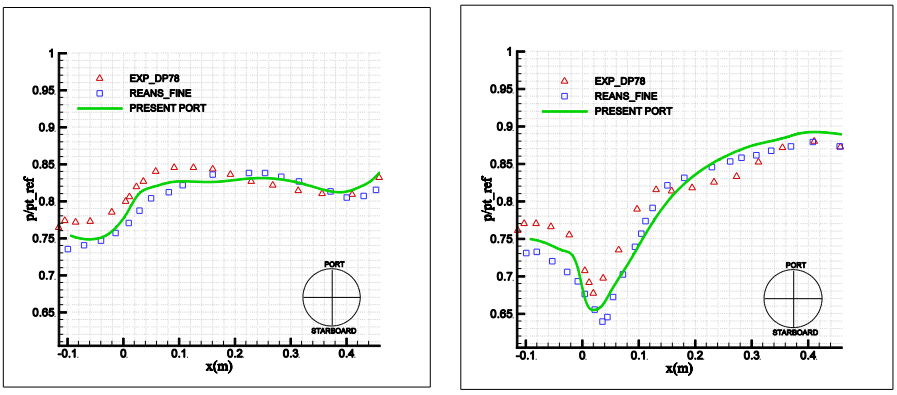

Fig. 3. Dimensionless pressure distribution along the side of the duct, port (Right), starboard (Left).

5. Comparison between the Cases with and Without VG

The aim of this study was to numerically analyse the improvement in the separation phenomenon using V.G. in internal flows. Therefore, the separation region had to be examined thoroughly in the flow prior to the installation of the VG. The reference Jin, Wonjin. (2008), which was published about the installation of V.G. in internal flows, suggested the use of transient flow conditions to allow for the observation of the separation region using conventional CFD techniques. Then, the V.G. had to be installed, and the improvement in a separation region was investigated. To better illustrate the beneficial effect of V.G in reducing the separation region, the first point is an inlet Mach number higher than 0.4, because for the inlet Mach numbers less than 0.4, according to empirical tests, V.G. is not required and

does not affect the flow. For this purpose, Boundary conditions are presented in Table 4 in Mach number of 0.87 Mohler Jr, S. R. (2004). Given the conditions mentioned above, first the vortex generator geometry is described, and then, all results are compared to the base case (without VG).

Table 4. Boundary and inlet Condition for S-duct According to "Mohler Jr, S. R. (2004)"

parameter	Value
M	0.78
α_1	0 Deg.
P_t	1011125 pa
T_t	287.2 k
P_s	66340 pa
T_s	255.97 k

6. Geometry of Parallel and Angled Blades (Vortex Generator)

To examine the effect of VG in reducing the flow separation region in a duct, two best arrangements were studied to be installed on the duct wall. The geometry parameters of the blades installed in the M2129 duct were selected according to Mohler Jr, S. R. (2004) and Anderson, B. H., & Gibb, J. (1998) for parallel arrangement and according to Paul, A. R. (2011) for angled arrangement Table 5 and Table 6 show the dimensions and the geometry of the blades in the parallel and angled arrangement, respectively. An example of the generated structured grid for the two case is shown in Fig. 4.

Table 5. Geometric dimensions of vortex generator with parallel Blades

t	α	L	h	h/c	C
0.05334	16 Deg.	1.778	0.4445	0.25	1.778

Table 6. Geometric dimensions of vortex generator with Angled Blades

t	β	l	h	h/c	C
0.05334	27 Deg.	1.778	0.4445	0.25	1.778

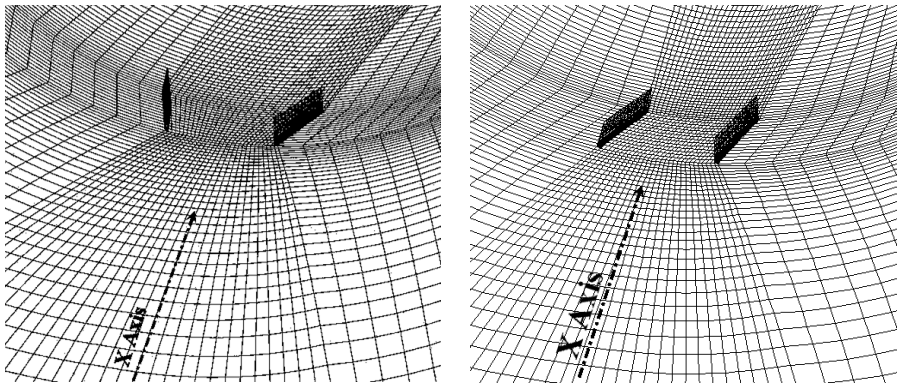

Fig. 4. Structured mesh of vortex generator with parallel and angled blades

7. Qualitative Comparison of Results in Different Sections

After investigating various geometries, blade arrangements, and computational grids, CFD simulation of flow was performed inside the duct for the three cases, i.e. base case (without VG), with parallel blade, and with angled blade according to the mentioned data and boundary conditions. The results of the parallel blade, which had the best total pressure recovery performance, were compared to those of the base case. It should be noted that in this section, the duct with the base geometry is in the right (a), and this with parallel blades is in the left (b).

Fig. 5 shows the total pressure contour in section 1 for the two above-mentioned cases. As previously mentioned, the location of the section 1 is approximately at the beginning of the separation region. This is clearly shown in Fig. 5(a). At bottom of the duct, pressure was reduced and reached about 82000 Pa. Fig. 5 (b) shows the total pressure contour in the same section in the case with parallel blades. As can be seen, a high amount of pressure in the region had been recovered, and the separation was practically reduced by a great extent in the region.

Fig. 6 and Fig. 7 show the total pressure contour in sections 2 and 3, respectively. As can be seen, in these areas, the total pressure in the case of parallel blades was greatly recovered, and the flow separation region was reduced. Consequently, in the section 3 and near the engine entrance, the total pressure drop in the worst area increased from 86000 (Pa) to 95000 (Pa) which could improve the total pressure recovery efficiency.

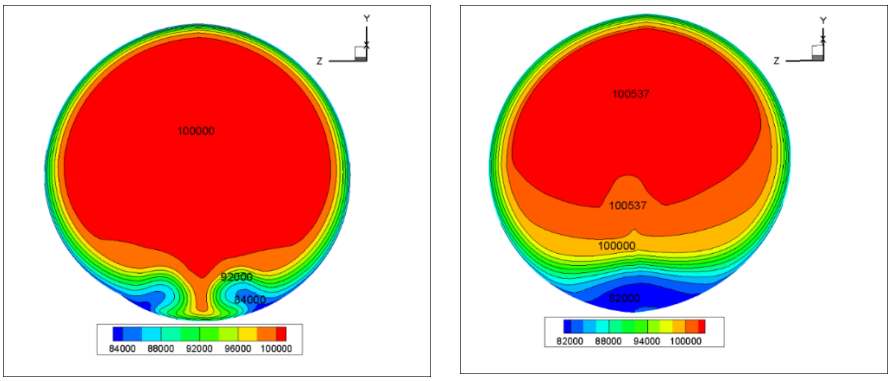

(a)-VG (b) +VG

Fig. 5. Total pressure contours with and without the parallel vortex generator at Sec.1

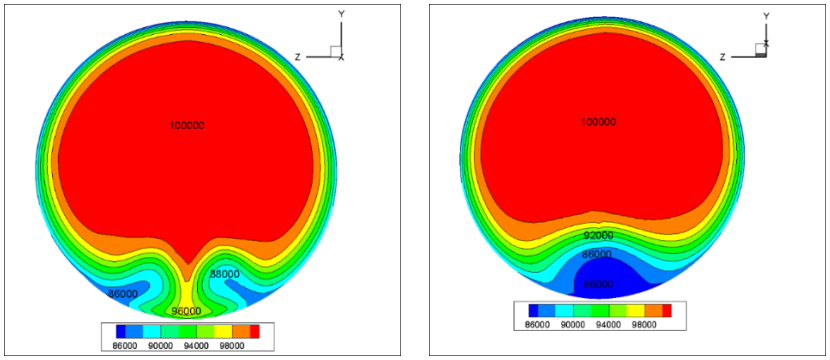

(a)-VG (b)+VG

Fig. 6. Total pressure contours with and without the parallel vortex generator at Sec.2

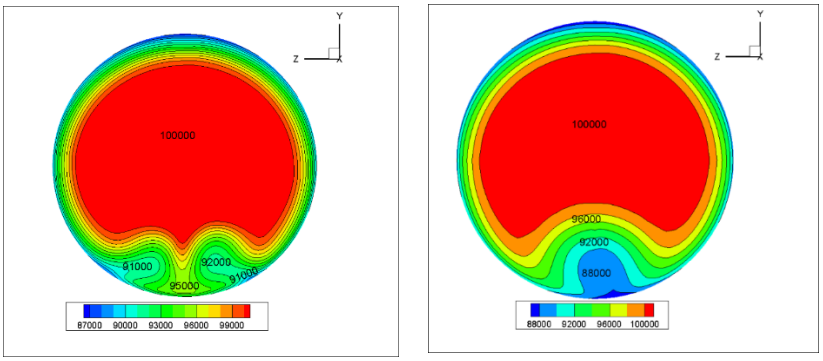

(a)-VG (b)+VG

Fig. 7. Total pressure contours with and without the parallel vortex generator at Sec.3

Fig. 8 shows the Mach number contour in the x-plane section and the perpendicular sections 1, 2, and 3. As can be seen, in Fig. 8 (a), the separation region can be clearly seen in the bottom area of the duct. Mach number between sections 1 and 2 dropped from 0.78 to 0.05, which shows a complete flow separation. In this case, the parallel blade compensated this phenomenon to a great extent, and the Mach number improved from 0.05 to 0.45 in this area.

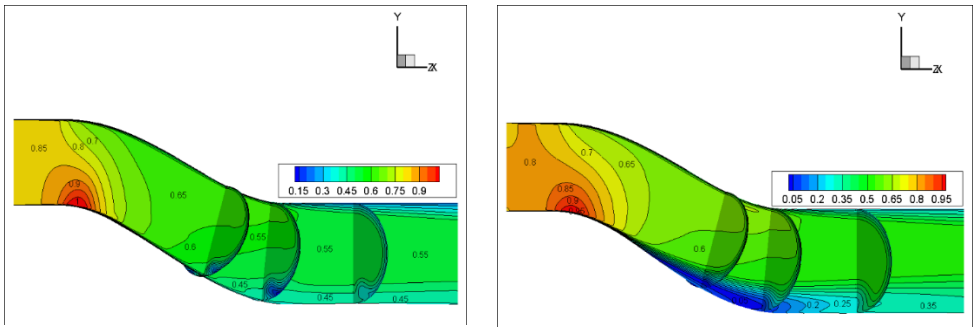

(a)-VG +(b)+VG

Fig. 8. Mach number contours with and without the parallel vortex generator along the flow direction

8. Quantitative Comparison of Results

In the previous section, the effects of installing VG was describes qualitatively. In this section, this phenomenon is compared quantitative between the three cases (base, parallel, and angled blade). According to Paul, A. R. (2011) and Ran, H. (2005), the most important parameter for evaluating the performance of an air intake duct is the total pressure recovery. According to the standard definitions, the total pressure recovery coefficient equals the average total pressure in the duct outlet (the plane of the engine entrance) divided by the average total pressure in the inlet plane. To better understand the numbers presented in the form of total pressure recovery, it should be noted that each 1% increase in the recovery coefficient increases the power of the engine connected to the duct by at least 1% Ran, H. (2005). Generally, in the real condition, a duct has a loss. Therefore, the recovery percentage of the duct pressure is expressed as follows:

$$\eta = 1 - \frac{\Delta P}{P_\infty} = 1 - \frac{P_i - P_f}{P_\infty} \tag{3}$$

In the literature, only less than 0.02 pressure drop of air intake is listed as the acceptable value. Therefore, a well-designed air intake duct must have a total pressure recovery percentage of over 98% Klausmeyer, S. M. (1996). The results of the numerical solution are shown in Table 7 according to the mentioned definition. The total pressure recovery increased significantly when vortex generator blades

were used inside the duct. The reason, as previously discussed, is the reduction in the separation region and the formation of a uniform flow in the outlet of the duct using the vortex generator blades. On the other hand, according to the arrangement of the blades on the duct wall, the pressure recovery was higher in the case of a parallel arrangement. Finally, using this type of blade, the total pressure recovery was increased from 96.65% to 97.08%.

Table 7. Total pressure Recovery along the duct with and without vortex generator

Types	P_{tai}	P_{tao}	η
-VG	101,125	97,741.32	96.65
+VGP	101,125	98,170.13	97.08
+VGA	101,125	98,146.31	97.05

9. Conclusion

An S-shaped air intake was studied in two cases of with and without a vortex generator. The vortex generator was placed at the upstream of the separation region in order to increase the momentum of the boundary layer and prevent the flow separation. The results of the vortex generator simulations, particularly the parallel blade, showed that compared with the base case, the total pressure recovery was increased from 96.65% to 97.08%, and the recovery percentage of duct pressure became close to the ideal value.

References

Guo, R. W., & Seddon, J. (1983). Swirl in an S-duct of typical air intake proportions, *Aeronautical Quarterly*, 34, 99-129.

Lin, J. C., Selby, G. V., & Howard, F. G. (1991). Exploratory study of vortex-generating devices for turbulent flow separation control, *AIAA Paper*, (1991-0042).

Reichert, B. A., & Wendt, B. J. (1993, January). An experimental investigation of S-duct flow control using arrays of low-profile vortex generators, *In 31st AIAA Aerospace Sciences Meeting and Exhibit*, vol. 1.

Reichert, B. A., & Wendt, B. J. (1994). Improving diffusing S-duct performance by secondary flow control, *National Aeronautics and Space Administration*.

Sullerey, R. K., Mishra, S., & Pradeep, A. M. (2002). Application of boundary layer fences and vortex generators in improving performance of S-duct diffusers, *Journal of fluids engineering*, 124(1), 136-142.

Berens, T.M., A.-L. Delot, and M. Chevalier (2012). Application of CFD to high offset intake diffusers, *GARTEUR TP–173*.

P. Spalart and S. Allmaras. (1992). A one-equation turbulence model for aerodynamic flows. *Technical Report AIAA-92-0439*, American Institute of Aeronautics and Astronautics.

Dacles-Mariani, J., Zilliac, G. G., Chow, J. S., & Bradshaw, P. (1995). Numerical/experimental study of a wingtip vortex in the near field, *AIAA journal*, 33(9), 1561-1568.

Jin, Wonjin. (2008). A Computational Study of Icing Effects on the Performance of an S-Duct Inlet, Ph.D. Thesis, University of Kansas.

Mohler Jr, S. R. (2004). Wind-US flow calculations for the M2129 S-duct using structured and unstructured grids, *AIAA Paper*, 525, 2004.

Anderson, B. H., & Gibb, J. (1998). Vortex-generator installation studies on steady-state and dynamic distortion, *Journal of Aircraft*, 35(4), 513-520.

Paul, A. R., Ranjan, P., Upadhyay, R. R., & Jain, A. (2011, May). Flow control in twin air-intakes using vortex generators, *In Proceedings of the 2011 international conference on Applied & computational mathematics*, World Scientific and Engineering Academy and Society (WSEAS), 107-116.

Ran, H., & Mavris, D. (2005, September). Preliminary design of a 2D supersonic inlet to maximize total pressure recovery, *In AIAA 5th Aviation, Technology, Integration and Operations Conference*, Virginia.

Klausmeyer, S. M., Papadakis, M., & Lin, J. C. (1996). A flow physics study of vortex generators on a multi-element airfoil, *AIAA Paper*, 96-0548.